Astron. Astrophys. 347, 720–723 (1999)

ASTRONOMY AND ASTROPHYSICS

Effects by sintering on the energy dissipation efficiency in collisions of grain aggregates

S. Sirono

Department of Earth and Planetary Sciences, Hokkaido University, Sapporo 060-0810, Japan (sirono@cosmos.sci.hokudai.ac.jp)

Received 15 January 1999 / Accepted 14 April 1999

Abstract. Energy dissipation on collisions of grain aggregates is investigated taking into account effects by sintering. It is shown that sintering significantly reduces the energy dissipation efficiency because contacts between adjacent grains become strong by sintering.

Key words: solar system: formation – ISM: dust, extinction

1. Introduction

Planetesimals, embryos of planets, are believed to be formed through coagulation of dust grains and their aggregates (e.g. Weidenschilling 1997) in a protoplanetary nebula rather than through gravitational instability proposed before (Goldreich & Ward 1973, Sekiya 1983).

Dominik & Tielens (1997) (hereafter DT97) performed numerical simulations of collisions between grain aggregates and showed that growth of aggregates made of astrophysically common materials, such as H_2O ice, graphite and silicates, is possible in the relevant conditions. Poppe et al. (1999) revealed experimentally that sticking threshold velocity of silicate grains to a wall is much higher than that predicted by Chokshi et al. (1993), suggesting that the growth of aggregates of silicate grains is more preferable than that expected from Chokshi et al. (1993). Poppe et al. (1999) concluded that there should be an additional energy dissipation mechanism other than damping of elastic waves investigated in Chokshi et al. (1993).

In all these works, grains are in contact by surface adhesion described by so-called JKR theory (Johnson 1985). Sintering, however, proceeds at contacts between dust grains at relevant conditions. It has been found experimentally (Supulver et al. 1997) that the sticking force of icy aggregates significantly increases by temperature increase. The sintering of H_2O ice seems to cause the increase of the sticking force, which is expected to lead to different collisional outcomes from those without sintering.

In this paper, we investigated numerically the amount of energy dissipation on collisions of grain aggregates taking into account effects by sintering. Basic processes of sintering are reviewed briefly in Sect. 2. Sect. 3 describes interactions between adjacent grains taking into account sintering. Numerical results are presented in Sect. 4.

Send offprint requests to: S. Sirono

2. Sintering processes

Fig. 1 shows a schematic view of a contact between adjacent grains. In this paper, it is assumed that an aggregate is composed of equal-sized spherical grains and we investigate collisions of aggregates made of H_2O ice. Initially, the grains are in contact by surface adhesion and a neck is formed as described by the JKR theory. Sintering proceeds as time and enlarges the neck seen in Fig. 1. The driving force of sintering is the difference in chemical potential between the neck and the other part of the grain. The chemical potential difference is originated from the difference in curvatures of the surfaces. In the relevant conditions considered here, surface diffusion of consisting molecules is the dominant process of sintering among six mechanisms (Swinkels & Ashby 1981). The elapsed time of sintering $\tau_{\rm sint}$ by the surface diffusion when the neck radius is grown to x is given by (Nichols & Mullins 1965)

$$\tau_{\rm sint} = \frac{x^6 kT}{25a^2 d\gamma\Omega D_{\rm s}}, \tag{1}$$

where a is the grain radius, γ is the surface energy, k is the Boltzmann constant, d and Ω is the size and volume of the molecule, and $D_{\rm s}$ is the surface diffusion coefficient of the molecule. The neck grows from $x/a = 1.2 \times 10^{-1}$ (determined from the JKR theory for H_2O ice, Johnson 1985) to $x/a = 0.8$ (the equilibrium value for an array of spheres, Nichols & Mullins 1965) according to Eq. (1). Strictly speaking, Eq. (1) is a formula approximating the numerical results of $x/a < 0.3$ (Nichols & Mullins 1965), nevertheless we can extrapolate Eq. (1) to $x/a = 0.8$ since the error is less than a factor of 2 and does not affect our discussion.

Putting values for H_2O ice to Eq. (1) as $d = 4.5 \times 10^{-8}\,\mathrm{cm}$, $\Omega = 3.25 \times 10^{-23}\,\mathrm{cm}^3$, $D_{\rm s} = 1.74 \times 10^5 \exp(-4590\,\mathrm{K}/T)\,\mathrm{cm}^2\,\mathrm{s}^{-1}$ (Kouchi et al. 1994), $\gamma = 100\,\mathrm{erg\,cm}^{-2}$ (Hobbs 1974), $a = 0.1\,\mu$m and $x/a = 0.8$ we obtain

$$\tau_{\mathrm{sint},\mathrm{H_2O}} = 1.8 \times 10^{-23} T \exp(4590\,\mathrm{K}/T)\,\mathrm{yr}. \tag{2}$$

For T =100 K, for example, Eq. (2) gives $\tau_{\mathrm{sint},\mathrm{H_2O}} = 0.15\,\mathrm{yr}$, which is sufficiently short time-scale compared to processes in

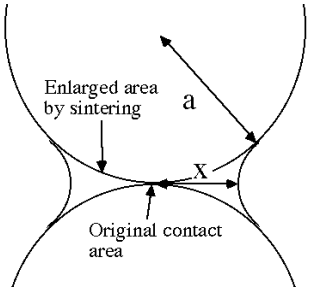

Fig. 1. A schematic view of a structure of a neck between adjacent dust grains.

a protoplanetary nebula such as Kepler time-scale showing that sintering will take place in a protoplanetary nebula.

3. Interactions between grains

Before sintering proceeds, the stretching motion between adjacent grains in contact are properly described by the JKR theory. Models of other modes of motions are discussed in DT97 including rolling, sliding and twisting, which are adopted here as the interactions before sintering takes place. The interactions before sintering are simplified in two points: 1) the stretching interaction is approximated as a linear spring kept separation energy of two grains constant and 2) dependences of the interactions on the neck radius are neglected. Simplification 1) presumably does not affect the results since DT97 has been revealed that the collisional outcomes are well classified in terms of the energy without use of the critical force for separating two grains. 2) is hold since the dependence is fairly weak (DT97). Correspondingly, all interactions between grains including that for sintered contacts are approximated by linear springs.

After sintering takes place, the spring constant k_h for stretching motion can be written by

$$k_{\rm h} = \frac{\pi\beta^2 aE}{2}, \tag{3}$$

where $\beta = 0.8$ (see Sect. 2) and E is the Young's modulus. We have approximated the sintered contact by a rod of radius βa. Likewise, the spring constants for rolling motion $k_{\rm r}$ and for sliding motion $k_{\rm s}$ are given by

$$k_{\rm r} = \frac{\pi\beta^4 a^3 E}{8} \tag{4}$$

$$k_{\rm s} = \frac{\pi\beta^2 aG}{2}, \tag{5}$$

where G is the shear modulus. When the stored elastic energy at the contact is equal to separation energy ($= 2\pi(\beta a)^2\gamma$) of the sintered contact, two grains are detached or start rolling (or sliding). The critical displacement ε_i for each motion denoted by i is determined by $k_i\varepsilon_i^2/2 = 2\pi(\beta a)^2\gamma$, leading to the expressions for the critical displacement for stretching $\varepsilon_{\rm h}$, for sliding $\varepsilon_{\rm s}$ and for rolling $\varepsilon_{\rm r}$ as

$$\varepsilon_{\rm h} = \sqrt{\frac{8\gamma a}{E}} \tag{6}$$

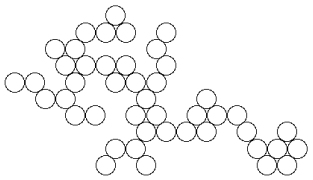

Fig. 2. An example of an initial configuration of an aggregate. Each grain has the same radius of $0.1\,\mu$m made of H_2O ice.

$$\varepsilon_{\rm s} = \sqrt{\frac{8\gamma a}{G}} \tag{7}$$

$$\varepsilon_{\rm r} = \sqrt{\frac{32\gamma}{\beta^2 Ea}}. \tag{8}$$

We adopted values for H_2O ice as $E = 7\times10^{10}\,{\rm dyn\,cm^{-2}}$, $G = 2.8\times10^{10}\,{\rm dyn\,cm^{-2}}$ (DT97) and the grain radius of $a = 0.1\,\mu$m. The spring constant of the stretching motion becomes strong by a factor of 17 due to sintering. For the rolling and sliding motion, the constants increase by a factor of 60 and 4, respectively. These increases cause the difference in the collisional outcomes of aggregates.

It should be noted that sintering changes the strength of a contact even before the enlargement of contact area due to sintering occurs. This is because stress developed around the JKR contact (non-sintered contact) will be relaxed by sintering. Only by this effect, the critical energy to initiate irreversible motion (cutting the springs) is increased by a factor of 1.0×10^4 for rolling, 1.3 for stretching and 2.4×10^{-2} for sliding with the use of the formulae obtained by DT97. The increase for the rolling motion is significant, because tensile stress developed near the perimeter of the JKR contact makes easy to start the rolling motion compared to a sintered contact. However, the energy decreases for the sliding motion, since compressive stress developed by the JKR contact contributing to oppose sliding will be relaxed by sintering.

4. Numerical results

We performed 2-D numerical simulations of collisions of grain aggregates. 2-D means that the motions of grains are restricted on a plane although each grain is treated as a 3-D object. Adjacent grains are connected by three linear springs corresponding three modes of motions described in the previous section. If the displacement exceeds the critical displacement of the spring, the spring is cut and elastic energy stored in the spring is dissipated. For rolling and sliding motion, the spring is connected again representing rolling and sliding friction. If one of three springs of a sintered contact is broken, all three springs are broken. A newly formed contact is assumed to be a non-sintered contact.

We simulated collisions of an aggregate to a wall, not between two aggregates, in order to concentrate on comparison of the amount of energy dissipation during the collisions before and after sintering takes place. In order to clarify *sticking probability* of aggregates, however, it is necessary to investigate effects by the configuration of grains relevant to the inter-penetration and

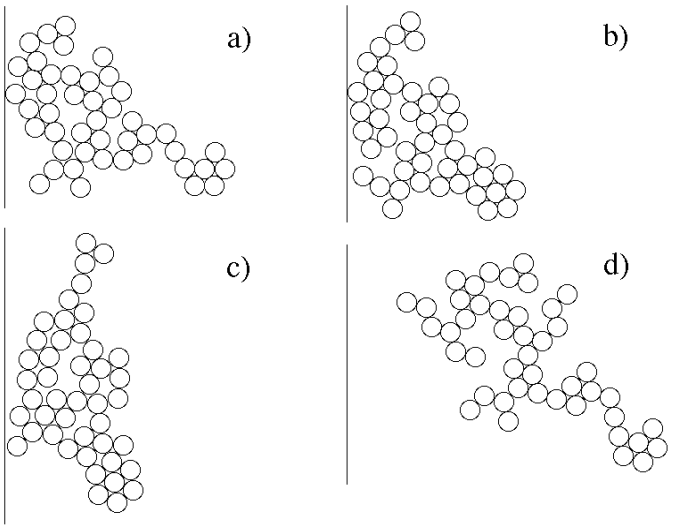

Fig. 3a–d. Snapshots of collision of an aggregate to a wall placed at leftmost. **a**, **b** and **c** are snapshots after collision of a non-sintered aggregate taken at 1.4×10^{-7} s, 2.7×10^{-7} s and 5.4×10^{-7} s, respectively. The impact velocity is $500\,\mathrm{cm\,s^{-1}}$. **d** is a snapshot of a sintered aggregate after bouncing taken at 1.4×10^{-7} s.

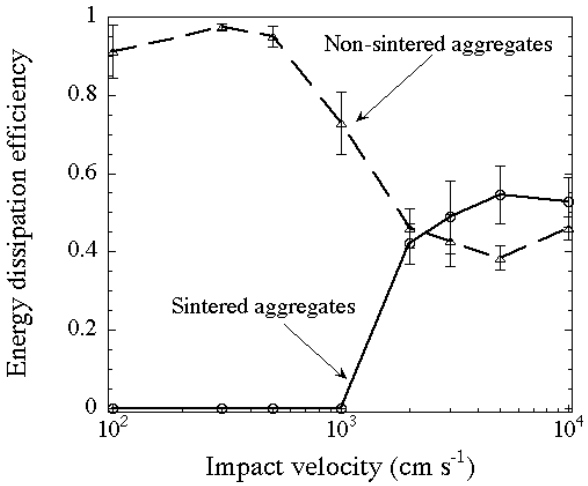

Fig. 4. The energy dissipation efficiency as a function of impact velocity. The solid line stands for the sintered aggregates and dashed line for the non-sintered aggregates. Error bars represent $1\,\sigma$ dispersions among four different initial configurations.

locking of the aggregates. This is beyond scope of this paper and will be treated in a forthcoming paper. It is assumed that there is no friction between the wall and grains.

Initial configurations of grains are produced by putting grains randomly on sites of 2-D triangular lattice. Numerical simulations are performed for four different initial configurations containing 43 to 48 grains. An example of the initial configuration is shown in Fig. 2.

Figs. 3 a) to c) show snapshots during a collision of a non-sintered aggregate with impact velocity of $500\,\mathrm{cm\,s^{-1}}$. The initial configuration of grains is that shown in Fig. 2. It can be seen that the re-arrangement of grains in the aggregate takes place. As the re-arrangement proceeds, more than 90% of initial kinetic energy is dissipated mostly by rolling friction. Varying the impact velocity, it has been confirmed that the outcomes of collisions (compaction, fragmentation, etc.) are properly classified by the ratio of initial kinetic energy to the critical energies for cutting the springs between grains as shown in DT97.

In the case of collisions of sintered aggregates, however, rearrangement of grains does not take place with impact velocity of $500\,\mathrm{cm\,s^{-1}}$ as shown in Fig. 3 d). The aggregate bounces from the wall without any energy dissipation at this impact velocity. This is simply because the strength of the contacts are increased by sintering and the aggregate can sustain the stress developed during the collision. The re-arrangement of grains in the sintered aggregates starts around impact velocity of $1200\,\mathrm{cm\,s^{-1}}$.

Fig. 4 summarizes the energy dissipation efficiency as a function of impact velocity. The energy dissipation efficiency is defined as one minus the ratio of energy stored in the aggregate after collision (kinetic+elastic energy) to the initial kinetic energy. Thus zero energy dissipation efficiency corresponds to no energy dissipation. When the impact velocity is less than $1000\,\mathrm{cm\,s^{-1}}$, sintered aggregates do not dissipate energy by the re-arrangement of grains in contrast to non-sintered aggregates, in which a significant fraction of initial kinetic energy is dissipated. Up to $2000\,\mathrm{cm\,s^{-1}}$, the efficiency for non-sintered aggregates exceeds that for the sintered aggregates. Above $2000\,\mathrm{cm\,s^{-1}}$, the efficiencies for sintered aggregates are slightly larger than that for non-sintered aggregates. According to Weidenschilling (1997), the maximum collision velocity of aggregates is about $1000\,\mathrm{cm\,s^{-1}}$. Therefore, sintering will affect the collisional outcomes in nebular conditions. Although the sticking probability should be investigated separately from this study, less energy dissipation efficiency of the sintered aggregates presumably leads to less sticking of the aggregates compared to non-sintered aggregates in a protoplanetary nebula.

As observed by Infrared Space Observatory satellite, ice in interstellar clouds contains not only H_2O but other species of ices such as CO and CO_2 (Whittet et al. 1996). Since temperature of sintering differs for each icy species, the existence of several species of ices may lead to formation of several separated regions in a protoplanetary nebula where sintering take place.

Finally, it should be pointed out the possibility that sintering proceeds further than that assumed in this paper. If this is the case, adjacent grains merge together beyond the formation of dendritic structure such as shown in Fig. 1. The strength of such a highly sintered aggregate should be higher than that studied here, leading to less energy dissipation efficiency than the results obtained in this paper.

Acknowledgements. The author is supported by Japan Society for the Promotion of Science (JSPS). The author greatly thanks to C. Dominik for his critical comments to the original manuscript.

References

Chokshi A., Tielens A.G.G.M., Hollenbach D., 1993, ApJ 407, 806

Dominik C., Tielens A.G.G.M., 1997, ApJ 480, 647 (DT97)
Goldreich P., Ward W.R., 1973, ApJ 183, 1051
Hayashi C., Nakazawa K., Nakagawa Y., 1985, In: Black D.C., Matthews M.S. (eds.) Protostars and Planets II. Univ. of Arizona Press, Tucson, p. 1100
Hobbs P.V., 1974, Ice Physics. Clarendon Press, Oxford
Johnson K.L., 1985, Contact mechanics. Cambridge Univ. Press, Cambridge
Kouchi A., Yamamoto T., Kozasa T., et al., 1994, A&A 209, 1009
Nichols F.A., Mullins W.W., 1965, J. App. Phys. 36, 1826
Poppe T., Blum J., Henning Th., 1999, Adv. Space Res., in press
Sekiya M., 1983, Prog. Theor. Phys. 69, 1116
Supulver K.D., Bridges F.G., Tiscareno S., et al., 1997, Icarus 129, 539
Swinkels F.B., Ashby M.F., 1981, Acta Metallurgica 29, 259
Weidenschilling S.J., 1997, Icarus 127, 290
Whittet D.C.B., Schutte W.A., Tielens A.G.G.M., et al., 1996, A&A 315, L357